

**BLOOD VESSEL AND RED LESION
SEGMENTATION FOR EARLY DIABETIC
RETINOPATHY SCREENING**

KAMINI UPADHYAY



**CENTRE FOR APPLIED RESEARCH IN ELECTRONICS
INDIAN INSTITUTE OF TECHNOLOGY DELHI**

OCTOBER 2022

© Indian Institute of Technology Delhi (IITD), New Delhi, 2022

**BLOOD VESSEL AND RED LESION
SEGMENTATION FOR EARLY DIABETIC
RETINOPATHY SCREENING**

by

KAMINI UPADHYAY

CENTRE FOR APPLIED RESEARCH IN ELECTRONICS

Submitted

in fulfillment of the requirements of the degree of Doctor of Philosophy

to the



**INDIAN INSTITUTE OF TECHNOLOGY DELHI
OCTOBER 2022**

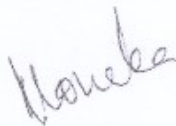
Dedicated to

My Family

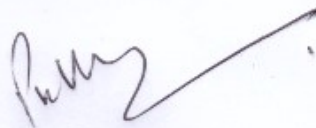
Certificate

This is to certify that the thesis entitled “**Blood Vessel and Red Lesion Segmentation for Early Diabetic Retinopathy Screening** ” being submitted by **Ms. Kamini Upadhyay** to the Centre for Applied Research in Electronics, Indian Institute of Technology Delhi, for the award of the degree of **Doctor of Philosophy** is the record of the bona-fide research work carried out by her under our supervision. In our opinion, the thesis has reached the standards fulfilling the requirements of the regulations relating to the degree.

The results contained in this thesis have not been submitted either in part or in full to any other university or institute for the award of any degree or diploma.



(Prof. Monika Aggarwal)
Centre for Applied Research in Electronics
Indian Institute of Technology Delhi
Hauz Khas, New Delhi 110016
India



(Prof. Praveen Vashist)
Community Ophthalmology
Dr RP Centre for Ophthalmic Sciences
AIIMS, New Delhi 110029
India

Acknowledgements

I would like to express my deep gratitude and thanks to a few people behind the successful completion of my doctoral dissertation. First of all, my sincere and deepest gratitude to my supervisors Prof. Monika Aggarwal and Prof. Praveen Vashist, for their valuable guidance, support, and consistent encouragement throughout my doctoral studies. Their motivation enabled me to come up with my original ideas, which helped me formulate meaningful research problems. Their profound technical knowledge, passion for research, attention to detail, and diligence helped shape my vision for future research. I am deeply indebted for their inspiration, motivation, and guidance.

I would also like to thank my student research committee members Prof. S.D. Joshi, Prof. Arun Kumar and Prof. R. Bahl for their useful interactions, invaluable comments, and suggestions. I am also thankful to all the professors at IIT Delhi from whom I had the opportunity to understand the fundamentals during the courses. I would also like to thank the staff members of the CARE office for taking care of all the paperwork and other logistics.

My stay at IIT Delhi would not have been so memorable without the friends I made along the journey. I am thankful to them for making my life joyful and being a constant source of encouragement. I also extend a big thanks to all the Ph.D. scholars of the signal processing group. They were always around to provide valuable suggestions, companionship and create a peaceful research environment.

Most importantly, I would like to acknowledge my parents Mr. Dinesh Upadhyay, Mrs. Omprabha Upadhyay, and my siblings Ms. Shivangi and Mr. Prabhanshu, for their unconditional love, continuous support, and blessings. My heartfelt thanks goes

out for my husband, Mr. Anurag, who was my true partner in every sense and stood by me through thick and thin times of this journey. His immense care, support and faith made my venture much easier. Last but not least, I feel truly blessed to have friends like Ms. Anuli and Ms. Sangeeta who always pushed me forward in my difficult times.

Kamini Upadhyay

Abstract

Diabetic Retinopathy (DR) is one of the significant causes of blindness amongst working-age adults throughout the world. It is an effect of prolonged Diabetes, which eventually weakens the retinal blood vessel walls, further leading into leakage of blood and other fluids into the eye. These leakages appear in the form of bright or red lesions in the retinal image. The disease progresses with changes in vessel structures, which in severe stages may cause irreversible damage to the retina.

Diagnosis of DR, especially in its early stages, can help in halting the progression of disease (by following proper clinical measures like, good control of blood sugar) and preserving the patient's vision. Moreover, if automated, then such tool can assist the medical experts for large scale, community-level screening.

In this thesis, we propose a segmentation-based approach to diagnose DR using 2-D fundus images. Here, we target the detection of initial symptoms of DR, which helps in DR diagnosis at any stage, including the challenging early stages. To begin with, we extract the retinal blood vessels, which is one of the most crucial and vulnerable features of a DR-affected retina. Though blood vessel is a typical feature of the retina, its segmentation is vital to understand the presence of abnormalities. We target this retinal vessel extraction in two ways. The first proposed method is unsupervised, based on conventional image processing techniques. In this pipe-line based method, we use multi-scaling (wavelets and curvelets) to target the varying width of blood vessels. This algorithm made us analyze and understand the fundus images in a subjective manner. Using the observed analysis of fundus images, we propose a combined approach in which the input fundus image is pre-processed in unsupervised manner and further fine-tuned to target vessel detection.

Red lesion based DR detection helps in screening out of DR patients even in the early stages. This is reportedly the initial abnormality that starts appearing on the retina due to swelling and leakage of blood from the retinal capillaries. We combine five handcrafted intensity features along-with deep-model extracted features to segment red lesions. Further, we use the presence of red lesions to predict the DR.

To summarize, the thesis proposes the extraction of retinal blood vessels and red lesions by analyzing 2-dimensional fundus images. Further, we use these extracted retinal features for the DR screening. We have explored various conventional image processing and deep learning methods to understand the retinal layer. Experimentation with a variety of datasets, has helped in developing robust and generic algorithms. The proposed screening algorithm is segmentation-based, which is more reliable and supposed to fill the gaps between machines and professionals by locating the abnormality. The analysis and observations stated in the thesis are meant to facilitate the medical community.

Abstract (सार)

डायबिटिक रेटिनोपैथी (डीआर) दुनिया भर में कामकाजी उम्र के वयस्कों में अंधेपन के महत्वपूर्ण कारणों में से एक है। यह लंबे समय तक चलने वाले मधुमेह का प्रभाव है, जो अंततः रेटिना की रक्त वाहिकाओं की दीवारों को कमजोर कर देता है, जिससे आगे चलकर रक्त और अन्य तरल पदार्थ आंखों में जाने लगते हैं। ये रिसाव रेटिना की छवि में चमकीले या लाल धावों के रूप में दिखाई देते हैं। रोग पोत संरचनाओं में परिवर्तन के साथ बढ़ता है, जो गंभीर चरणों में रेटिना को अपरिवर्तनीय क्षति का कारण बन सकता है।

डीआर का निदान, विशेष रूप से इसके प्रारंभिक चरण में, रोग की प्रगति को रोकने में मदद कर सकता है (उचित नैदानिक उपायों जैसे, रक्त शर्करा के अच्छे नियंत्रण का पालन करके) और रोगी की दृष्टि को संरक्षित करने में मदद कर सकता है। इसके अलावा, यदि स्वचालित है, तो ऐसे उपकरण बड़े पैमाने पर, सामुदायिक स्तर की जांच के लिए चिकित्सा विशेषज्ञों की सहायता कर सकते हैं।

इस थीसिस में, हम 2-डी फंडस छवियों का उपयोग करके डीआर का निदान करने के लिए एक विभाजन-आधारित दृष्टिकोण का प्रस्ताव करते हैं। यहां, हम डीआर के शुरुआती लक्षणों का पता लगाने का लक्ष्य रखते हैं, जो चुनौतीपूर्ण प्रारंभिक चरणों सहित किसी भी स्तर पर डीआर निदान में मदद करता है। शुरू करने के लिए, हम रेटिना की रक्त वाहिकाओं को निकालते हैं, जो डीआर-प्रभावित रेटिना की सबसे महत्वपूर्ण और कमजोर विशेषताओं में से एक है। हालांकि रक्त वाहिका रेटिना की एक विशिष्ट विशेषता है, लेकिन असामान्यताओं की उपस्थिति को समझने के लिए इसका विभाजन महत्वपूर्ण है। हम इस रेटिना पोत निष्कर्षण को दो तरह से लक्षित करते हैं। पारंपरिक छवि प्रसंस्करण तकनीकों के आधार पर पहली प्रस्तावित विधि पर्यवेक्षित नहीं है। इस पाइप-लाइन आधारित पद्धति में, हम रक्त वाहिकाओं की अलग-अलग चौड़ाई को लक्षित करने के लिए मल्टी-स्केलिंग (वेवलेट्स और कर्वलेट) का उपयोग करते हैं। इस एल्गोरिथम ने हमें एक व्यक्तिपरक तरीके से फंडस छवियों का विश्लेषण और समझने में मदद की। फंडस छवियों के देखे गए विश्लेषण का उपयोग करते हुए, हम एक संयुक्त दृष्टिकोण का प्रस्ताव करते हैं जिसमें इनपुट फंडस छवि को पूर्व-संसाधित किया जाता है और पोत का पता लगाने को लक्षित करने के लिए फाईने-ट्यून किया जाता है।

लाल धाव-आधारित डीआर का पता लगाने से प्रारंभिक अवस्था में भी डीआर रोगियों की जांच करने में मदद मिलती है। यह कथित तौर पर प्रारंभिक असामान्यता है जो रेटिना पर सूजन और रेटिना केशिकाओं से रक्त के रिसाव के कारण दिखाई देने लगती है। हम लाल धावों को खंडित करने के लिए गहरे-मॉडल निकाले गए सुविधाओं के साथ-साथ पांच दस्तकारी तीव्रता सुविधाओं को जोड़ते हैं। इसके अलावा, हम डीआर की भविष्यवाणी करने के लिए लाल धावों की उपस्थिति का उपयोग करते हैं।

संक्षेप में, थीसिस 2-आयामी फंडस छवियों का विश्लेषण करके रेटिना रक्त वाहिकाओं और लाल धावों के निष्कर्षण का प्रस्ताव करती है। इसके अलावा, हम डीआर स्क्रीनिंग के लिए इन निकाले गए रेटिना सुविधाओं का उपयोग करते हैं। हमने विभिन्न पारंपरिक छवि की खोज की है | रेटिनल लेयर को समझने के लिए प्रोसेसिंग और डीप लर्निंग मेथड्स। विभिन्न प्रकार के डेटासेट के साथ प्रयोग ने मजबूत और सामान्य एल्गोरिदम विकसित करने में मदद की है। प्रस्तावित स्क्रीनिंग एल्गोरिथम विभाजन-आधारित है, जो अधिक विश्वसनीय है और असामान्यता का पता लगाकर मशीनों और पेशेवरों के बीच की खाई को भरना चाहिए। थीसिस में वर्णित विश्लेषण और अवलोकन चिकित्सा समुदाय की सुविधा के लिए हैं।

Table of Contents

Acknowledgements	i
Abstract	iii
List of Figures	ix
List of Tables	xvi
Abbreviations	xviii
1 Introduction	1
1.1 Medical Image Analysis	1
1.2 Diabetic Retinopathy	2
1.2.1 Clinical Features	3
1.2.2 Stages of Diabetic Retinopathy	5
1.2.3 Retinal Imaging	5
1.3 Motivation	7
1.4 Diabetic Retinopathy Screening	8
1.4.1 Fundus Image Dataset	8
1.4.2 Unsupervised Vessel Segmentation	9
1.4.3 Supervised Vessel Segmentation	10
1.4.4 Red Lesion Segmentation and DR Screening	11
1.5 Contribution of the Thesis	12
1.6 Organization of the Thesis	13

2	Unsupervised Retinal Blood Vessel Segmentation	15
2.1	Introduction	15
2.2	Proposed Method for Unsupervised Vessel Extraction	19
2.2.1	Pre-processing	20
2.2.2	Core processing : Gray-scale Vessel Enhancement	23
2.2.3	Post-processing	32
2.3	Materials and Metrics	32
2.4	Experiments and Discussions	35
2.4.1	Results	35
2.4.2	Discussions	40
2.5	Chapter Summary	43
3	Supervised Retinal Blood Vessel Segmentation	45
3.1	Introduction	45
3.2	Algorithm I	48
3.2.1	Pre-processing	49
3.2.2	Wavelet-based Vessel Enhancement	49
3.2.3	Supervised Fine-Tuning	49
3.3	Algorithm II	50
3.3.1	Pre-processing	51
3.3.2	Multi-level Vessel Enhancement	51
3.3.3	Supervised Fine-Tuning	54
3.4	Algorithm III	55
3.4.1	Pre-processing	56
3.4.2	Adaptive Multi-scale Analysis	56
3.4.3	Deep learning for Multi-scale Analysis	60
3.5	Experiments and Discussions	63
3.5.1	Datasets	63
3.5.2	Evaluation metrics	63
3.5.3	Discussion	63

3.6	Chapter Summary	67
4	Red Lesion Segmentation and DR Detection	71
4.1	Introduction	71
4.2	Red lesion segmentation and DR screening	75
4.2.1	Pre-processing	76
4.2.2	Patch extraction	76
4.2.3	Handcrafted feature extraction	78
4.2.4	Training	80
4.2.5	DR Screening	81
4.3	Material and Metrics	82
4.3.1	Dataset	82
4.3.2	Performance metrics	83
4.4	Experiments and Discussions	84
4.5	Chapter Summary	90
5	Conclusion and Future Work	92
5.1	Conclusion	92
5.2	Future Work	94
	Bibliography	95
	List of Publications	104
	Technical Biography of Author	105

List of Figures

1.1	<i>Illustration of some medical imaging modalities: X-ray, CT, fundus, ultrasound, MRI from left to right. [Source : www.wikipedia.com]</i> . . .	1
1.2	<i>Simulation result of Normal vision versus DR affected vision. The person with DR has a blurred view with floating patches. [Source-http://www.efei.com/diabetic-eye-disease]</i>	3
1.3	<i>Illustration of normal and abnormal features in retina : (a) Healthy retina with optic disc, blood vessels, and macula; (b) Retina with microaneurysms and hemorrhages (red lesions), (c) Retina with hard and soft exudates (bright lesions), (d) Retina with neovascularisation.</i> . . .	4
1.4	<i>Illustration of multiple stages of DR. The chart mentions the associated visible clinical features at each stage. [Source-Author's own]</i>	5
1.5	<i>(a)A non mydriatic, digital fundus camera, Topcon TRC NW8 [Source-https://www.digitaleyecenter.com], (b) Illustration of 2-D projection of retina visible to the ophthalmologist [Source-https://www.ucl.ac.uk/ioo/research/research-labs-and-groups/carr-lab/bestrophinopathies-resource-pages/eye/retina-and-retinal]</i>	7
2.1	<i>Block diagram of the proposed unsupervised vessel segmentation algorithm. The diagram shows three major blocks: pre-processing (RoI extraction, color normalization, green channel extraction), core-processing (CWT, DCuT, morphological thickness correction), and post-processing (thresholding, morphological opening, pruning)</i>	17

2.2	<i>Illustration of derived binary masks from example RGB fundus images</i> : (a) ‘01_test’ from DRIVE, (b) ‘im0077’ from STARE, (c) ‘Image_05L’ from CHASE_DB-1, (d) ‘08_dr’ from HRF dataset.	22
2.3	<i>Color normalization</i> : (a) ‘01_test’ image from DRIVE dataset as input, (b) ‘im0077’ image from STARE dataset as reference, (c) Output fundus after matching input to the reference.	23
2.4	<i>Top-hat transformation on green channel sub-image $I_{3,2}(x, y)$ from ‘01_test’ of DRIVE dataset</i> : (a) Green channel sub-image, (b) Inverted green channel sub-image, (c) Top-hat transformed sub-image.	25
2.5	<i>Magnitude of maximum of real response of the sub-image $I_{3,2}(x, y)$ from ‘01_test’ of DRIVE dataset at different scales</i> : (a) $a_1 = 1$, (b) $a_2 = 2$, (b) $a_3 = 3$, (b) $a_4 = 4$	27
2.6	<i>Illustration of contrast enhancement using DCuT</i> : (a) Combined wavelet response image, $I_M^\psi(x, y)$, (b) Coarsest version of wavelet response im- age, $D_L(x, y)$, (c) Remaining image containing the details, $I_C(x, y)$, (d) Resulting contrast-enhanced image, $I_{VE}(x, y)$	29
2.7	<i>Background texture removal</i> : (a) Contrast enhanced vessel map ob- tained using DCuT, $I_{VE}(x, y)$, (b) Thin vessel map obtained after re- moving non-vessel background texture, $I_{thin}(x, y)$	29
2.8	<i>Gray-scale Morphological extraction of major vessel arcade</i> : (a) Inverted green channel image, (b) Contrast enhanced image, (c) Image after Mor- phological opening, (d) Top-hat transformation of contrast enhanced image.	31
2.9	<i>Vessel-width correction</i> : (a) $I_{thin}(x, y)$, (b) $I_{thick}(x, y)$, (c) $I_{vessel}(x, y)$	32
2.10	<i>Post-processing steps</i> : (a) Output binary vessel map, (b) Vessel map after morphological area opening, (c) Vessel map after morphological pruning.	33

2.11	<i>Comparison of the output vessel segmentation on image ‘01_test’ from DRIVE dataset using the proposed method and the nearest best performing method Orlando et al. [41]. The obtained vessel map is shown in green w.r.t. the ground truth in red. The color coding facilitates in viewing the missed vessels. The proposed method has been successful in extracting the complete vessel map except some very fine vessel ends, visible in red. The other method is observed to be missing out on fine vessels. (a) Result of proposed method, (b) Result of nearest best method.</i>	36
2.12	<i>Comparison of mean ROC curves of proposed algorithm on different datasets.</i>	37
2.13	<i>Comparative vessel segmentation results on sample pathological images, ‘14_test’ from DRIVE and ‘im0044’ from STARE datasets. The proposed method shows a promising vessel extraction even in the presence of red lesions on DRIVE data image, as it has not misidentified the red lesions as vessels, as done by the nearest best method [41]. The sample STARE image has challenging bright region where the proposed method has been successful in extracting a better continuous vessel map and fine vessels as compared to the nearest best method [33]: (a,b,c) Comparison on DRIVE image, (d,e,f) Comparison on STARE image.</i>	38
2.14	<i>Comparative vessel segmentation results on sample pathological images, ‘Image_05L’ from CHASE_DB-1 and ‘07_dr’ HRF datasets. The proposed algorithm has been successful in extracting vessel maps, including the thin vessels, even in challenging fundus background. The image from CHASE_DB-1 has in-homogeneous illumination, the proposed method has successfully extracted some very fine poor-contrast vessels, whereas the other method [45] could not perform well in such regions. In HRF image, many fine vessels are missed by the nearest best method [50] in comparison to the proposed method: (a,b,c) Comparison on CHASE_DB-1 image, (d,e,f) Comparison on HRF image.</i>	39

2.15	<i>Illustration of failure of proposed algorithm in case of dominant choroidal vessels : (a) Example fundus image ‘23_training’ of DRIVE dataset, (b) Segmented vessel map in green w.r.t. the ground truth.</i>	41
3.1	<i>Block diagram of the proposed vessel extraction using algorithm-I. Here, we process input color fundus images to extract corresponding three channel images, with the magnitude of real wavelet transform coefficients corresponding to different scales in each channel. These images are used to train U-net for vessel extraction.</i>	48
3.2	<i>Magnitude of maximum real response at different scales for image ‘im0077’ of STARE data-set : (a) $a=2$, (b) $a=3$, (c) $a=4$, (d) Final concatenated image shown in RGB colorspace.</i>	50
3.3	<i>Block diagram of the proposed vessel extraction using algorithm-II. Here, we propose two parallel pipelines, CWT and Gaussian matched filtering to enhance vessels at multiple levels. The texture suppression preserving the vessel edges, is done at each level and we extract the common maximum response for each pixel. U-net is further used for fine-tuning.</i>	51
3.4	<i>Vessel Enhancement using Gabor Wavelet at different scales : (a) $a=1$, (b) $a=2$ (c) $a=3$; Texture Removal at different scales : (d) $a=1$, (e) $a=2$, (f) $a=3$</i>	52
3.5	<i>Gaussian Matched Filtering at different spreads : (a) $\sigma=1$, (b) $\sigma=2$ (c) $\sigma=3$; Corresponding Texture Removal at each variance : (d) $\sigma=1$, (e) $\sigma=2$ (f) $\sigma=3$</i>	53
3.6	<i>Pipeline of the proposed Vessel Extraction using Deep-fusion of Multi-scale Features. The pipeline is composed of three major steps: Pre-processing, Adaptive Gabor Decomposition, and Deep learning for multi-scale analysis.</i>	55
3.7	<i>Illustration of pre-processing of input data : (a) Input RGB image ‘16_test’ from DRIVE, (b) Green channel, (c) Binary FoV mask, (d) Extracted RoI and (e) CLAHE enhanced image.</i>	56

3.8	<i>Bar graph between the correlation coefficient and scale parameter for different databases. It is clear that signal's energy is focused in only a few scales, which can be considered as the most significant ones.</i>	58
3.9	<i>Specific patch extraction from four challenging regions of fundus image: partially inside OD, near bright illuminations, partially inside FoV, and poorly illuminated regions.</i>	61
3.10	<i>The proposed U-net architecture for vessel segmentation using wavelet based multi-scale feature maps.</i>	62
3.11	<i>ROC plot for the four different databases. Curves are deviating very slightly which prove the consistent thus robust performance of the proposed algorithm.</i>	67
3.12	<i>Qualitative comparison of vessel segmentation on DRIVE database : (a) RGB image '16_test', (b) Ground truth, (c) Our predicted vessel map, (d) Vessel map predicted by Orlando et al. [41], (e) Vessel map predicted by Li et al. [39]</i>	68
3.13	<i>Qualitative comparison of vessel segmentation on STARE database : (a) RGB image 'im65', (b) Ground truth, (c) Our predicted vessel map, (d) Vessel map predicted by Liskowski [33], (e) Vessel map predicted by Li et al. [39].</i>	68
3.14	<i>Qualitative comparison of vessel segmentation on CHASE_DB-1 database : (a) RGB image 'Image_01L', (b) Ground truth, (c) Our predicted vessel map, (d) Vessel map predicted by Jin et al. [74], (e) Vessel map predicted by Li et al. [39].</i>	69
3.15	<i>Qualitative comparison of vessel segmentation on HRF database : (a) RGB image '11_H', (b) Ground truth, (c) Our predicted vessel map, (d) Vessel map predicted by Yan et al. [50], (e) Vessel map predicted by Li et al. [39].</i>	69
4.1	<i>A typical example of presence of red lesions on the retina. MAs and HEMs are marked in red and green color, respectively.</i>	72

4.2	<i>Block diagram of the proposed red-lesion segmentation algorithm illustrating three major blocks: pre-processing, training patch extraction, integration of handcrafted features to the deep model.</i>	74
4.3	<i>Illustration of pre-processing steps applied for input image enhancement : (a) Input RGB fundus image, (b) Vessel map inpainting to enhance red lesions, (c) Green channel extraction for best visualization of red lesions on fundus background, (d) Contrast enhancement using CLAHE to obtain final pre-processed image.</i>	76
4.4	<i>Illustration of the deep model used for the proposed red lesion segmentation. Here, we use an encoder decoder based U-net architecture with concatenation of handcrafted feature map in the end.</i>	78
4.5	<i>An Ablation study to understand the individual contribution of different steps in the proposed approach. It considers three steps: 1. Random patch-based training of baseline U-net, 2. Random patch-based training of U-net with concatenated handcrafted feature map, 3. Characteristic patch-based training of U-net with concatenated handcrafted feature map.</i>	83
4.6	<i>The Precision-Recall (PR) curve for red lesion segmentation on IDRiD and DDR datasets.</i>	86
4.7	<i>Illustration of red lesion segmentation on sample images from IDRiD database. (a, b, c, d): Input color fundus images; (e, f, g, h): Segmentation results for proposed method; (i, j, k, l): Segmentation results for Guo et al. [82]. In the segmentation results, the predicted lesions are shown in green, and ground truth in red color. The yellow pixels show the obtained true positives. The red pixels are the false negatives, i.e. the missed lesions. The proposed lesion segmentation is clearly outperforming the nearest best performing method.</i>	87

4.8 Illustration of red lesion segmentation on sample images from DDR database. (a, d): Input color fundus images; (b, e): Segmentation results for proposed method; (c, f): Segmentation results for Guo et al. [68]. In the segmentation results, the predicted lesions are shown in green, and ground truth in red color. The yellow pixels show the obtained true positives. The red pixels are the false negatives, i.e. the missed lesions. 88

List of Tables

1.1	Fundus image datasets used in this work	9
2.1	Performance of proposed algorithm on image ‘01_test’ from DRIVE dataset (a healthy fundus)	36
2.2	Performance of proposed algorithm on some pathological images of publicly available datasets w.r.t. Expert-1 (in case, more than one expert annotations available)	38
2.3	Performance comparison of proposed algorithm on DRIVE and STARE datasets	42
2.4	Performance comparison of proposed algorithm on CHASE_DB-1 and HRF datasets	42
3.1	Fundus image datasets used in the proposed algorithm	59
3.2	Step-wise contribution of the proposed method (DRIVE)	63
3.3	Performance comparison of proposed algorithm on DRIVE	64
3.4	Performance comparison of proposed algorithm on STARE	64
3.5	Performance comparison of proposed algorithm on CHASE_DB-1	65
3.6	Performance comparison of proposed algorithm on HRF	66
3.7	Cross-database performance of proposed algorithm	67
4.1	Performance comparison for proposed segmentation of red lesions with other recent methods	85
4.2	Performance comparison of the proposed method with finalists of IDRiD grand challenge (<i>Source : https://idrid.grand-challenge.org/Leaderboard/</i>)	85

4.3	Comparison of the proposed DR screening with other recent methods . . .	90
-----	---	----

Abbreviations

2-D	2-Dimensional
Acc	Accuracy
AMD	Age-related Macular Degeneration
AUC	Area Under the Curve
AUPR	Area Under Precision Recall curve
CHASE_DB	Child Heart and Health Study in England Database
CLAHE	Contrast Limited Adaptive Histogram Equalization
CNN	Convolutional Neural Network
CT	Computerized Tomography
CWT	Continuous Wavelet Transform
DCuT	Discrete Curvelet Transform
DDR	Dataset of Diabetic Retinopathy
DM	Diabetes Mellitus
DL	Deep Learning
DR	Diabetic Retinopathy
DRIVE	Digital Retinal Images for Vessel Extraction
FCN	Fully Convolutional Network
FoV	Field-of-View
FP	False Positive
FPR	False Positive Rate
FN	False Negative
GAN	Generative Adversarial Networks

GMM	Gaussian Mixture Model
HEM	Hemorrhages
HE	Hard Exudates
HRF	High Resolution Fundus
IDRiD	Indian Diabetic Retinopathy Image Dataset
IRMA	Intra-Retinal Microvascular Abnormality
kNN	k-Nearest Neighbour
LLF	Local Laplacian Filter
MA	Microaneurysms
MCC	Matthews Correlation Coefficient
MF	Matched Filtering
MF-FDOG	Matched Filtering-First Order Derivative of Gaussian
ML	Machine Learning
mPR	mean Precision Recall
MRI	Magnetic Resonance Imaging
NPDR	Non Proliferative Diabetic Retinopathy
OD	Optic Disc
PDR	Proliferative Diabetic Retinopathy
Pr	Precision
Re	Recall
ReLU	Rectified Linear Unit
RGB	Red Green Blue
ROC	Receiver Operating Characteristic curve
RoI	Region of Interest
RoP	Retinopathy of Prematurity
RL	Red Lesion
Sen	Sensitivity
SGD	Stochastic Gradient Descent
Spe	Specificity

STARE STructured Analysis of the Retina
SVM Support Vector Machine
TP True Positive
TPR True Positive Rate
TN True Negative